HHS Public Access

Author manuscript

J Bone Miner Res. Author manuscript; available in PMC 2023 December 07.

Published in final edited form as:

J Bone Miner Res. 2007 September ; 22(9): 1329–1337. doi:10.1359/jbmr.070517.

IGF-I Receptor Is Required for the Anabolic Actions of Parathyroid Hormone on Bone

Yongmei Wang[1], **Shigeki Nishida**[1], **Benjamin M Boudignon**[1], **Andrew Burghardt**[2], **Hashem Z Elalieh**[1], **Michelle M Hamilton**[1], **Sharmila Majumdar**[2], **Bernard P Halloran**[1], **Thomas L Clemens**[3], **Daniel D Bikle**[1]

[1]Department of Medicine, Endocrine Unit, Veterans Affairs Medical Center, and University of California, San Francisco, California, USA;

[2]Department of Radiology, University of California, San Francisco, California, USA;

[3]Division of Molecular and Cellular Pathology, Department of Pathology, University of Alabama at Birmingham, Birmingham, Alabama, USA.

Abstract

We showed that the *IGF-IR*–null mutation in mature osteoblasts leads to less bone and decreased periosteal bone formation and impaired the stimulatory effects of PTH on osteoprogenitor cell proliferation and differentiation.

Introduction: This study was carried out to examine the role of IGF-I signaling in mediating the actions of PTH on bone.

Materials and Methods: Three-month-old mice with an osteoblast-specific *IGF-I* receptor null mutation (IGF-IR OBKO) and their normal littermates were treated with vehicle or PTH (80 μg/kg body weight/d for 2 wk). Structural measurements of the proximal and midshaft of the tibia were made by μCT. Trabecular and cortical bone formation was measured by bone histomorphometry. Bone marrow stromal cells (BMSCs) were obtained to assess the effects of PTH on osteoprogenitor number and differentiation.

Results: The fat-free weight of bone normalized to body weight (FFW/BW), bone volume (BV/TV), and cortical thickness (C.Th) in both proximal tibia and shaft were all less in the IGF-IR OBKO mice compared with controls. PTH decreased FFW/BW of the proximal tibia more substantially in controls than in IGF-IR OBKO mice. The increase in C.Th after PTH in the proximal tibia was comparable in both control and IGF-IR OBKO mice. Although trabecular and periosteal bone formation was markedly lower in the IGF-IR OBKO mice than in the control mice, endosteal bone formation was comparable in control and IGF-IR OBKO mice. PTH stimulated endosteal bone formation only in the control animals. Compared with BMSCs from control mice, BMSCs from IGF-IR OBKO mice showed equal alkaline phosphatase $(ALP)^+$ colonies on day 14, but fewer mineralized nodules on day 28. Administration of PTH increased the number of ALP^+

Address reprint requests to: Daniel D Bikle, MD, PhD, Endocrine Unit (111N), VAMC 4150 Clement Street San Francisco, CA 94121, USA, daniel.bikle@ucsf.edu.

The authors state that they have no conflicts of interest.

colonies and mineralized nodules on days 14 and 28 in BMSCs from control mice, but not in BMSCs from IGF-IR OBKO mice.

Conclusions: Our results indicate that the *IGF-IR* null mutation in mature osteoblasts leads to less bone and decreased bone formation, in part because of the requirement for the *IGF-IR* in mature osteoblasts to enable PTH to stimulate osteoprogenitor cell proliferation and differentiation.

Keywords

PTH; IGF-I signaling; osteoprogenitor; proliferation; bone formation rate

INTRODUCTION

PTH IS A major regulator of calcium and phosphate homeostasis. Although it has been well established that PTH exerts both anabolic[1,2] and catabolic[3,4] actions on bone in animals and humans, the mechanism is unclear. The bone marrow stromal cells (BMSCs)/osteoblasts have been shown to be the primary target cells for actions of PTH on bone. PTH binds to a seven membrane-spanning G protein–coupled receptor (PTH/PTHrP receptor) on the surface of stromal cells/osteoblasts and activates both the cAMP protein kinase A (PKA) and phosphoinositide protein kinase C (PKC) pathways. When given intermittently, PTH increases bone mass and strength by increasing the number[5] or function of osteoblasts[6] and by inhibiting osteoblast apoptosis[7,8] (anabolic effect). Continuous infusion of PTH leads to bone loss by stimulating a net increase in bone resorption[3,4] through an increase in the gene expression ratio of RANKL/osteoprotegerin (OPG) (catabolic effect). These effects are both direct actions of PTH on osteoblast lineage cells and indirect through modulation of local growth factor production. In particular, IGF-I has been shown to be an important mediator for the anabolic actions of PTH on bone.[9,10]

Previous studies indicated that the IGF-I system plays a key role in bone metabolism. It acts in diverse patterns, through a combination of endocrine, autocrine, and paracrine modes of action, to regulate the functions of both osteoblasts and osteoclasts.[11–13] Signaling through the IGF-I receptor (IGF-IR), which is expressed in bone cells, not only promotes osteoblast proliferation and/or differentiation but also mediates anti-apoptotic actions.[14,15] PTH stimulates IGF-I production by bone cells, and antibodies to IGF-I can block the actions of PTH on bone. When PTH was administered to global *IGF-I* knockout mice, anabolic actions of PTH on bone were suppressed.[9,10] Although all of these previous studies indicated the importance of IGF-I in mediating the anabolic actions of PTH, the mechanisms by which IGF-I mediates the actions of PTH on bone and the function of IGF-IR in mediating these actions remain poorly understood. Because of complex relationships in the signaling processes of IGF-I regulation,[16,17] the complex effects of PTH on bone, and the poor survival rate of global *IGF-I*–null mice,[18] it has been difficult to define individual in vivo aspects of the skeletal actions of IGF-I as a mediator of bone actions of PTH. Compared with mice with global IGF-I–null mutations[18] and global IGF-I receptor (*IGF-IR*)–null mutations,[19] mice with *IGF-IR*–null mutations specifically in osteoblasts[14] have a normal survival. As such, these mice provide us with a new tool to study the role of IGF-I signaling in mediating the skeletal actions of PTH.

MATERIALS AND METHODS

Animals

IGF-IR OBKO mice were generated by crossing homozygous conditional mutants carrying modified *IGF-IR* alleles (with *loxP* sites flanking exon3)[20] with mice carrying the cre recombinase transgene under the control of an osteocalcin promoter.[14] These mice were normal in survival rate, body size, and weight. Twelve-week-old control mice and mice with an osteoblast-specific *IGF-IR*–null mutation were treated with either PTH [lsqb]PTH(1–34), rat; Bachem[rsqb] 80 μg/kg body weight (BW) or vehicle (150 mM NaCl, 1 mM 1 N HCl, and 2% heat-inactivated FBS dissolved in distilled water) everyday by subcutaneous injection for 2 wk. Each group contained equal numbers of male and female mice. To determine both trabecular and cortical bone formation during the period of PTH administration, the mice were injected subcutaneously with fluorochrome (each 15 mg/kg) on day 0 (the day PTH administration was started) (calcein), day 6 (demeclocycline), and day 12 (calcein) of PTH administration to label the mineralization fronts of the bone. Two days later, the mice were weighed and killed. The right tibias were obtained for fat-free weight, μCT, cortical bone mineral appositional rate (MAR), and bone formation rate (BFR) at the tibiofibular junction (TFJ). The right distal femurs were obtained for trabecular bone histomorphometry. To determine the effect of PTH on BMSC differentiation and mRNA levels of bone markers, the mice were killed 1 h after the last PTH treatment. Left tibias and femurs were obtained for mRNA determinations. BMSCs from left tibias and femurs were collected individually for cell culture. These studies were approved by the Animal Use Committee of the San Francisco Veterans Affairs Medical Center where the animals were raised and studied.

Fat-free weight

The tibias were cleaned of adherent tissue, extracted in ethanol and diethyl ether using a Soxhlet apparatus (Fisher Scientific, Pittsburgh, PA, USA), dried at 100°C overnight, and weighed.

μCT

The tibias were analyzed with a Scanco Medical AG μCT apparatus (Scanco Medical, Basserdorf, Switzerland) as previously described.[9,21,22] 3D information was obtained by stacking successively measured slices on top of each other. The voxel size was 9 μm in all three spatial dimensions. One hundred twenty-eight slices were measured in each sample, covering a total of 1.15 mm of the metaphysis. To analyze only cancellous fractions of the tibias, the compact part of the bone was masked out in the following way: with a 3D box-shaped low-pass filter applied to the original gray-scale CT images, an artificial partial volume effect was created, which blurs out the individual trabeculae but leaves the dense compact shell intact. The cortex mask was extracted with a simple thresholding operation with a fixed threshold of 20.0% of the maximal grayscale value. To analyze the cortex, a low-pass Gaussian filter (s = 3.0) was applied to the original images, with a threshold of 10.0%. The axial position and extent are identical to the trabecular volume. The trabecular region was masked out, and a 3D component labeling of the cortex was performed additionally to extract only the main connected component. The cortex was evaluated with

the direct distance transformation method to calculate its thickness. Bone volume (BV) and bone surface (BS) were calculated using a tetrahedron meshing technique generated with the marching cubes method. Total volume (TV) was calculated from the volume of the conforming voxels of interest (VOIs).

Histomorphometry

Trabecular bone: Right distal femurs were dehydrated in graded ethanol solutions and xylene and embedded undecalcified in modified methyl methacrylate.[23] These bone samples were sectioned longitudinally with a Leica RM 2165 microtome at indicated thicknesses of 8–10 μm. The 8-μm sections were stained with modified Goldner trichrome protocol to determine trabecular bone volume, whereas the 10-μm sections remained unstained for dynamic measurements of bone formation by assessing the labeling by demeclocycline and the second calcein injection (6-day interval).

Histomorphometric data were collected using the Bioquant Bone Morphometry System (Nashville, TN, USA) and reported according to standard bone histomorphometry nomenclature.[24]

Cortical bone: Diaphyseal segments of the right tibias were dehydrated, defatted in acetone followed by ether, and embedded in bioplastic (Tap Plastics, Dublin, CA, USA). After polymerizing overnight, the blocks were sectioned at a thickness of 60 μm using a Leica SP 1600 circular bone saw (Leica, Deerfield, IL, USA). The section containing the TFJ was digitized with a Hamamatsu video camera (Carl Zeiss, Thornwood, NY, USA) coupled to a Leica DMR microscope, and periosteal and endosteal MAR and BFR were determined using the NIH Image program (BFR and MAR were measured by assessing the two calcein labels (12-day interval).

BMSC culture

The left tibial and femoral BMSCs were harvested using techniques previously described.[25] Briefly, the tibias and femurs were collected, the soft tissue, and the epiphyses of each bone were removed. The bone marrow was flushed from the diaphysis with a syringe and a 26-gauge needle. The marrow from each individual mouse was collected in primary culture medium (α-MEM; containing L-glutamine and nucleosides; Mediatech, Herndon, VA, USA), supplemented with 10% FBS (Atlanta Biologicals, Norcross, GA, USA), 100 U/ml penicillin/streptomycin (Mediatech), and 0.25 μg/ml fungizone (Life Technologies, Rockville, MD, USA). A single-cell suspension was obtained by repeated passage through an 18-gauge needle. A pool of BMSCs was made from the tibia and femur of each mouse. The cells were plated at 10×10^6 cells/dish in 10-cm dishes. Nonadherent cells were removed by aspiration, and the primary medium was replenished on day 5. On day 7, the cells were provided with secondary medium (the primary medium with 3 mM β-glycerophosphate and 50 μg/ml ascorbic acid; Sigma, St Louis, MO, USA). Subsequent medium changes were performed every 2 days for up to 28 days.

Determination of alkaline phosphatase–positive colony number and calcium nodule formation

BMSCs were grown in 10-cm dishes for up to 28 days. At day 14 of culture, cells were assessed using a commercial kit (diagnostics kit, procedure no. 86; Sigma) to determine alkaline phosphatase $(ALP)^+$ colony-forming units (CFUs) following the manufacturer's instructions. At day 28 of culture, calcium nodules were stained with Alizarin red (AR; Sigma) for 10 min, the stain was aspirated, and the dishes were rinsed five times by distilled water to remove loosely bound stain. The number of mineralized nodules was determined, and the specifically bound stain was eluted with a solution of 0.5 N HCl/5% SDS and quantitated in a spectrophotometer at 415 nm.

Quantitative real-time PCR

RNA was extracted from the long bones (bone marrow flushed out) of control and IGF-IR OBKO mice. mRNA levels of osteoblast differentiation markers were determined by quantitative real-time PCR as previously described.[9] Primers and probes are as follows: *GAPDH* (forward: 5′-TGCACCACCAACTGCTTAG-3′; reverse: 5′-GGATGCAGGGATGATGTTC-3′; probe: 5′-CAGAAGACTGTGGATGGCCCCTC-3′), *RUNX2* (forward:5′- GGCTCTGGCGTTTAAATGGTT-3′; reverse: 5′-GTGCCCTCTGTTGTAAATACTGCTT-3′; probe: 5′-CCACCGAGACCAACCGAGTCATTTAAGG-3′), *ALP* (forward: 5′-TCCTGACCAAAAACCTCAAAGG-3′; reverse: 5′-TGCTTCATGCAGAGCCTGC-3′; probe: 5′- CTGGTGGAAGGAGGCAGGATTGACC-3′), *osteocalcin* (forward: 5′-CTCACAGATGCCAAGCCCA-3; reverse: 5′-CAAGGTAGCGCCGGAGTCT-3′; probe: 5′- CCCTGAGTCTCTGACAAAGCCTTCATGTCCA-3′), and *RANKL* (forward: 5′-GGCCACAGCGCTTCTCAG-3′; reverse: 5′-GAGTGACTTTATGGGAACCCGAT-3′; probe: 5′-CAGCTATGATGGAAGGCTCATGGTTGGA-3′).

Statistical analysis

Data are presented as mean ± SD. All data were analyzed using two-factor (genotype and treatment) ANOVAs followed by a posthoc Fisher's protected least significant difference (PLSD) test with a SuperANOVA program. Statistical significance was stated for $p < 0.05$.

RESULTS

BMC

The fat-free weights of tibias (normalized by body weight, FFW/BW) are shown in Fig. 1. By one-way ANOVA analysis, in vehicle-treated mice, FFW/BW of IGF-IR OBKO mice (1.21 ± 0.11 mg/g) was significantly lower than FFW/BW of control mice (1.44 ± 0.12 mg/g; $p = 0.001$). PTH significantly decreased FFW/BW by 10% in control mice (1.32 ± 0.13 mg/g; $p = 0.02$) but had less effect in IGF-IR OBKO mice (1.12 ± 0.09 mg/g; $p = 0.06$). Two-way ANOVA revealed a significant PTH treatment-*IGF-IR* gene mutation interaction ($p < 0.05$).

Bone structure: proximal tibia

μCT was used to evaluate the effects of PTH on bone structure of control and IGF-IR OBKO. The field of interest was the secondary spongiosa. The results are shown in Fig. 2. In IGF-IR OBKO mice, cortical bone thickness (C.Th) was significantly less than in control mice (Fig. 2B). PTH significantly decreased bone volume (BV, 30%; Fig. 2A) and increased C.Th (Fig. 2B) in control mice, but induced no significant changes in IGF-IR OBKO mice, although the trend was comparable.

Bone histomorphometry

Trabecular bone at primary and secondary spongiosa: We first determined whether the IGF-IR is required for PTH stimulation of bone formation in trabecular bone. As shown in Fig. 3, trabecular bone volume (BV/TV) was significantly decreased (33%, $p < 0.05$) in the primary spongiosa of the IGF-IR OBKO mice (Figs. 3A3 and 3B) than in the control mice (Figs. 3A1 and 3B). PTH stimulated BV/TV (50%, $p < 0.05$) in the primary spongiosa of the control mice (Figs. 3A2 and 3B), but had less effect in the IGF-IR OBKO mice (Figs. 3A4 and 3B). On the other hand, at the secondary spongiosa, PTH showed no effects on BV/TV (Fig. 3C) in either control or IGF-IR OBKO mice. In the secondary spongiosa, both single-labeled surfaces (sLS) and doublelabeled surfaces (dLS) tended to be lower in the IGF-IR OBKO (sLS: 653.4 ± 70.6 μm; dLS: 326.7 ± 35.3 μm) compared with the control mice (sLS: 962.0 ± 102.2 μm; dLS: 960.1 ± 202.6 μm). In the control mice, PTH showed no significant effects on sLS (973.6 ± 184.6 μm) or dLS (1313.6 ± 254.3 μm). In IGF-IR OBKO mice, PTH increased dLS (1112.1 ± 190.2 μm), but induced no changes on sLS (983.6 ± 209.8 μm). Trabecular bone formation rate/bone surface (BFR/BS) in the IGF-IR OBKO mice was 48% ($p < 0.05$) lower than that in the control mice (Fig. 3D). PTH stimulated BFR/BS by 114% ($p < 0.05$) in control mice and 85% ($p < 0.05$) in IGF-IR OBKO mice (Fig. 3D), although the absolute increase in BFR/BS in the IGF-IR KO mice was substantially less than controls owing to the lower basal levels of BFR/BS. There were no differences in the MAR between the control mice and the IGF-IR OBKO mice. PTH increased MAR by 52% ($p < 0.05$) in control mice but had no effect in the IGF-IR OBKO mice (Fig. 3E).

Cortical bone at tibiofibular junctions: We determined whether the IGF-I receptor is needed for PTH stimulation of bone formation at the TFJ by bone histomorphometry. The results are shown in Fig. 4. Periosteal BFR (Fig. 4A) and MAR (Fig. 4B) at the TFJ were markedly lower in the IGF-IR OBKO mice than in the control mice. PTH treatment increased periosteal BFR (40%, $p = 0.058$; Fig. 4A) and MAR (40%, $p = 0.058$; Fig. 4B) at the TFJ in control mice, but not in IGF-IR OBKO mice. Endosteal BFR (Fig. 4C) and MAR (Fig. 4D) were comparable in control and IGF-IR OBKO mice, but PTH stimulated endosteal BFR (76%) and MAR (76%) only in the control animals ($p < 0.05$; Figs. 4C and 4D).

Osteoblast progenitor proliferation and mineralization

On day 14 of BMSC culture (Fig. 5A), the numbers of ALP^+ colonies formed in the cultures from the IGF-IR OBKO mice (122 ± 12) and the control mice (124 ± 21) were equivalent.

However, PTH administration in vivo significantly increased the number of ALP^+ colonies (160 ± 24) in BMSC cultures subsequently obtained from control mice (129% of vehicle treated control mice, $p < 0.05$; Fig. 5A), but induced no changes in that from IGF-IR OBKO mice. On day 28 of BMSC culture (Fig. 5B), the number of mineralized nodules in the cultures from the IGF-IR OBKO mice (100 ± 9) was significantly less ($p < 0.05$) than that observed in the cultures from the control mice (164 ± 19; Fig. 5B). This progressive loss of differentiation capacity in the IGF-IR OBKO was accompanied by a progressive loss of *IGF-IR* expression in vitro. On day 14 of BMSC culture, the mRNA level of *IGF-IR* in the IGF-IR OBKO cells was 75%, whereas on day 28 of BMSC culture, it decreased to 38% of the control cells (data not shown). The mRNA levels of *IGF-IR* in the control cells remained constant between days 14 and 28 (data not shown). Administration of PTH in vivo increased the number of mineralized nodules 1.5-fold in BMSC cultures subsequently obtained from control mice (from 164 ± 19 to 246 ± 8, $p < 0.05$), but not in BMSC cultures from IGF-IR OBKO mice (Fig. 5B; from 100 ± 9 to 122 ± 12). Two-way ANOVA showed a significant interaction between PTH and *IGF-IR* genotype on the number of mineralized nodules ($p = 0.03$).

mRNA levels of bone markers

The mRNA levels of selected bone markers in extracts of intact bone were determined by quantitative real-time PCR. The results are shown in Table 1. These values are expressed as a percentage of *GAPDH* expression. The mRNA levels of *IGF-I* were significantly higher in the IGF-IR OBKO mice than in the control mice. PTH significantly increased the mRNA levels of *IGF-I* (1.5-fold) in the control mice but induced no changes in the IGF-IRKO mice. The mRNA levels of *RUNX2, ALP*, and *RANKL* were equivalent in the control mice and the IGF-IR OBKO mice, but the mRNA levels of *osteocalcin* were significantly lower in the IGF-IR OBKO mice than in control mice. PTH significantly increased the mRNA levels of *RUNX2, ALP, osteocalcin*, and *RANKL* in the control mice (4.9-, 5.5-, 5.7-, and 23.7-fold, respectively), but not in IGF-IR OBKO mice. The interactions between PTH and *IGF-IR* genotype on the expression of these genes were significant (two-way ANOVA).

DISCUSSION

PTH has complex effects on bone, not all of which are direct. IGF-I is an attractive candidate as a mediator for at least some of these actions. In this study, we determined the effects of PTH on a mouse model in which the floxed type *I IGF-IR* gene was selectively deleted in mature osteoblasts using an osteocalcin promoter driven cre-recombinase (IGF-IR OBKO). Previous studies[14] showed that the IGF-IR OBKO mice were normal in size and body weight but had lower trabecular bone volume, connectivity, trabecular number, mineralization rate, and an increased trabecular spacing, findings that we confirmed in this study. In this study, we further showed that the *IGF-IR*–null mutation in mature osteoblasts, not only affected trabecular bone but also cortical bone formation and mineralization. The lower periosteal bone formation rate and mineralization at the TFJ resulted in decreased cortical bone thickness, which together with the abnormalities in trabecular bone, resulted in a lower FFW/BW. At the cellular level, we observed that the *IGF-IR*–null mutation in mature osteoblasts did not affect the osteoprogenitor numbers, as indicated by ALP^+

CFUs, but markedly reduced their differentiation into mineralized nodules. These results are consistent with the loss of *IGF-IR* as the osteoblasts differentiate in vitro, turning on the osteocalcin driven cre recombinase that inactivates the floxed *IGF-IR* gene in late stage cultures. At the molecular level, the *IGF-IR*–null mutation in mature osteoblasts did not affect the mRNA levels of early osteoblast differentiation markers *RUNX2* and *ALP*, but decreased the mRNA levels of the late osteoblast differentiation marker *osteocalcin*, consistent with the failure of the osteoprogenitor cells from the IGF-IR OBKO mice to fully differentiate.

The major question we addressed in this study was whether the actions of PTH on bone were altered in the IGF-IR OBKO mice. Consistent with the results from earlier studies,[26,27] PTH increased trabecular bone, but in this study, this anabolic action was confined to the primary spongiosa. That PTH had a greater anabolic effect in this region may be caused by the greater expression of *IGF-I* in the osteoblasts of the primary spongiosa.[28] Deletion of *IGF-IR* in the mature osteoblasts blunted the anabolic effects of PTH on BV/TV, indicating that *IGF-IR* in mature osteoblasts was involved in mediating the anabolic actions of PTH on trabecular bone at the primary spongiosa. On the other hand, in the secondary spongiosa, as shown by other investigators,[29] PTH stimulated BFR and MAR, but induced no changes in trabecular bone volume in either control or IGF-IR OBKO mice. This may be because of differences in the balance between anabolic and catabolic actions of PTH in the primary and secondary spongiosa, perhaps because of reduced IGF-I expression or differences in structure between primary and secondary spongiosa. For example, there are fewer bone surfaces on which new bone formation can occur in the secondary spongiosa. It also may be that, in our study, 2 wk of PTH administration was not long enough to maximize the anabolic effects of PTH in the secondary spongiosa. The deletion of *IGF-IR* in mature osteoblasts did not completely block the stimulatory effects of PTH on BFR in trabecular bone as it did in cortical bone. Unlike bone histomorphometry, but consistent with our earlier studies,[9,30] μCT measurements of the secondary spongiosa indicated that PTH had catabolic effects on trabecular bone. Because FFW/BW showed decreased mineral content in the PTH-treated groups, this may have led to an underestimation of BV by μCT. Our data, together with that from other studies, suggest that μCT measurements should also be performed of the primary spongiosa. In the diaphysis, the periosteal and endosteal osteoblasts also express high levels of IGF-I.[28,31] As analyzed by BFR, MAR, and bone structural changes, PTH increased endosteal and periosteal bone formation and mineralization and increased cortical bone thickness. As seen in trabecular bone, the anabolic effects of PTH on cortical were blunted in the IGF-IR OBKO mice. Here the lack of anabolic effects of PTH in the IGF-IR OBKO was more pronounced, showing the importance of IGF-I signaling in the mature osteoblast for mediating the anabolic actions of PTH on bone.

BMSCs/osteoblasts play central roles in directing the anabolic and catabolic effects of PTH on bone.[6,32] At the cellular level, the anabolic effects of PTH may be attributed to several different mechanisms such as increasing the total number of osteoprogenitor cells[5] or inhibiting apoptosis.[7,33] In this study, we analyzed the effects of PTH given in vivo on BMSC proliferation and differentiation in vitro, and found that PTH increased both ALP^+ colony number and mineralization in the cultures from the control mice. These

findings support the concept that PTH acts by increasing the number of osteoprogenitor cells. However, our observation that deletion of the *IGF-IR* from the mature osteoblast blocks the ability of PTH to increase the numbers of ALP^+ colonies suggests that this action of PTH is indirect (i.e., mediated by the mature osteoblast). Depending on the different protocols[5,7,33] and animal models used, previous studies have shown inconsistent results in the effect of PTH on cell proliferation. Using a rat model, Nishida et al.[5] showed that 3 wk of PTH administration (30 μg/kg body weight) increased ALP^+ colony number at day 13 of BMSC cultures. In contrast, using mouse models, Knopp et al.[33] and Jilka et al.[7] showed that 4 wk of PTH administration at a dose of 95 or 400 μg/kg body weight, respectively, did not increase the number of ALP^+ colonies at day 21[33] or day 28[7] of BMSC cultures, but extended the life span of osteoblasts, resulting in an increase in bone deposition with time. Our data support the concept that the anabolic effects of PTH are caused by increased osteoprogenitors that differentiate into osteoblasts to form more bone. However, our data do not exclude an effect on PTH on enhanced osteoblast survival. At the molecular level, PTH stimulated the expression of *IGF-I* in the control mice, which would act as an autocrine/paracrine factor to stimulate osteoblast proliferation and differentiation. PTH also stimulated the expression of *RUNX2* and *ALP*, two early stage osteoblast differentiation markers, and *osteocalcin*, a late stage osteoblast differentiation marker, consistent with its effects on BMSC differentiation. PTH also stimulated the expression of *RANKL*. RANKL binds to its receptor RANK on the surface of osteoclast precursors, initiates osteoclastogenesis,[34–36] leading to the catabolic actions of PTH on bone.[3,37] In the BMSC cultures from the IGF-IR OBKO mice, as indicated by the measurement of ALP^+ colony number, the loss of *IGF-IR* in mature osteoblasts blunted the stimulatory effects of PTH given in vivo on osteoprogenitor cell proliferation measured in vitro. Similarly, loss of *IGF-IR* in mature osteoblasts blocked the stimulatory effects of PTH given in vivo on the gene expression of early (*RUNX2, ALP*) and late (*osteocalcin*) osteoblast differentiation markers in bone, and osteoblast differentiation and mineral matrix production in vitro. Finally, the loss of *IGF-IR* in mature osteoblasts blocked the stimulatory effects of PTH given in vivo on *RANKL* expression in bone, thus blunting the catabolic effects of PTH on mineral content. We conclude that IGF-I signaling in mature osteoblasts mediates both the anabolic effects of PTH on bone by inducing osteoprogenitor cell proliferation and differentiation and the catabolic effects of PTH by inducing *RANKL* expression. The *IGF-IR* in the mature osteoblast is needed for these PTH stimulated events to occur. The mechanism for this is unclear but is under active study in our laboratory.

In summary, our results indicate that the *IGF-IR* in mature osteoblasts is needed both for normal bone remodeling and for PTH responsiveness of both mature osteoblasts and osteoblast progenitors. The later may be affected secondarily perhaps by PTH-stimulated IGF-I production from mature osteoblasts, but the precise role of the *IGF-IR* in the mature osteoblast in mediating these actions of PTH remains for future study.

ACKNOWLEDGMENTS

This work was supported by grants from the National Institutes of Health RO1 DK 54793 and the National Aeronautic and Space Administrations NN04CC67G.

REFERENCES

1. Dempster DW, Cosman F, Kurland ES, Zhou H, Nieves J, Woelfert L, Shane E, Plavetic K, Muller R, Bilezikian J, Lindsay R 2001 Effects of daily treatment with parathyroid hormone on bone microarchitecture and turnover in patients with osteoporosis: A paired biopsy study. J Bone Miner Res 16:1846–1853. [PubMed: 11585349]
2. Alexander JM, Bab I, Fish S, Muller R, Uchiyama T, Gronowicz G, Nahounou M, Zhao Q, White DW, Chorev M, Gazit D, Rosenblatt M 2001 Human parathyroid hormone 1–34 reverses bone loss in ovariectomized mice. J Bone Miner Res 16:1665–1673. [PubMed: 11547836]
3. Ma YL, Cain RL, Halladay DL, Yang X, Zeng Q, Miles RR, Chandrasekhar S, Martin TJ, Onyia JE 2001 Catabolic effects of continuous human PTH (1–38) in vivo is associated with sustained stimulation of RANKL and inhibition of osteoprotegerin and gene-associated bone formation. Endocrinology 142:4047–4054. [PubMed: 11517184]
4. Lee SK, Lorenzo JA 1999 Parathyroid hormone stimulates TRANCE and inhibits osteoprotegerin messenger ribonucleic acid expression in murine bone marrow cultures: Correlation with osteoclast-like cell formation. Endocrinology 140:3552–3561. [PubMed: 10433211]
5. Nishida S, Yamaguchi A, Tanizawa T, Endo N, Mashiba T, Uchiyama Y, Suda T, Yoshiki S, Takahashi HE 1994 Increased bone formation by intermittent parathyroid hormone administration is due to the stimulation of proliferation and differentiation of osteoprogenitor cells in bone marrow. Bone 15:717–723. [PubMed: 7873302]
6. Rubin MR, Cosman F, Lindsay R, Bilezikian JP 2002 The anabolic effects of parathyroid hormone. Osteoporos Int 13:267–277. [PubMed: 12030541]
7. Jilka RL, Weinstein RS, Bellido T, Roberson P, Parfitt AM, Manolagas SC 1999 Increased bone formation by prevention of osteoblast apoptosis with parathyroid hormone. J Clin Invest 104:439–446. [PubMed: 10449436]
8. Bellido T, Ali AA, Plotkin LI, Fu Q, Gubrij I, Roberson PK, Weinstein RS, O'Brien CA, Manolagas SC, Jilka RL 2003 Proteasomal degradation of Runx2 shortens parathyroid hormone-induced anti-apoptotic signaling in osteoblasts. A putative explanation for why intermittent administration is needed for bone anabolism. J Biol Chem 278:50259–50272. [PubMed: 14523023]
9. Bikle DD, Sakata T, Leary C, Elalieh H, Ginzinger D, Rosen CJ, Beamer W, Majumdar S, Halloran BP 2002 Insulin-like growth factor I is required for the anabolic actions of parathyroid hormone on mouse bone. J Bone Miner Res 17:1570–1578. [PubMed: 12211426]
10. Miyakoshi N, Kasukawa Y, Linkhart TA, Baylink DJ, Mohan S 2001 Evidence that anabolic effects of PTH on bone require IGF-I in growing mice. Endocrinology 142:4349–4356. [PubMed: 11564695]
11. Rosen CJ 2004 Insulin-like growth factor I and bone mineral density: Experience from animal models and human observational studies. Best Pract Res Clin Endocrinol Metab 18:423–435. [PubMed: 15261847]
12. Yakar S, Rosen CJ 2003 From mouse to man: Redefining the role of insulin-like growth factor-I in the acquisition of bone mass. Exp Biol Med (Maywood) 228:245–252. [PubMed: 12626768]
13. Clemens TL, Chernausek SD 2004 Genetic strategies for elucidating insulin-like growth factor action in bone. Growth Horm IGF Res 14:195–199. [PubMed: 15125880]
14. Zhang M, Xuan S, Bouxsein ML, von Stechow D, Akeno N, Faugere MC, Malluche H, Zhao G, Rosen CJ, Efstratiadis A, Clemens TL 2002 Osteoblast-specific knockout of the insulin-like growth factor (IGF) receptor gene reveals an essential role of IGF signaling in bone matrix mineralization. J Biol Chem 277:44005–44012. [PubMed: 12215457]
15. Zhao G, Monier-Faugere MC, Langub MC, Geng Z, Nakayama T, Pike JW, Chernausek SD, Rosen CJ, Donahue LR, Malluche HH, Fagin JA, Clemens TL 2000 Targeted overexpression of insulin-like growth factor I to osteoblasts of transgenic mice: Increased trabecular bone volume without increased osteoblast proliferation. Endocrinology 141:2674–2682. [PubMed: 10875273]
16. Le Roith D, Bondy C, Yakar S, Liu JL, Butler A 2001 The somatomedin hypothesis: 2001. Endocr Rev 22:53–74. [PubMed: 11159816]
17. McCarthy TL, Centrella M 2001 Local IGF-I expression and bone formation. Growth Horm IGF Res 11:213–219. [PubMed: 11735236]

18. Powell-Braxton L, Hollingshead P, Warburton C, Dowd M, Pitts-Meek S, Dalton D, Gillett N, Stewart TA 1993 IGF-I is required for normal embryonic growth in mice. Genes Dev 7:2609–2617. [PubMed: 8276243]
19. Liu JP, Baker J, Perkins AS, Robertson EJ, Efstratiadis A 1993 Mice carrying null mutations of the genes encoding insulin-like growth factor I (Igf-1) and type 1 IGF receptor (Igf1r). Cell 75:59–72. [PubMed: 8402901]
20. Dietrich P, Dragatsis I, Xuan S, Zeitlin S, Efstratiadis A 2000 Conditional mutagenesis in mice with heat shock promoterdriven cre transgenes. Mamm Genome 11:196–205. [PubMed: 10723724]
21. Bikle D, Majumdar S, Laib A, Powell-Braxton L, Rosen C, Beamer W, Nauman E, Leary C, Halloran B 2001 The skeletal structure of insulin-like growth factor I-deficient mice. J Bone Miner Res 16:2320–2329. [PubMed: 11760848]
22. von Stechow D, Zurakowski D, Pettit AR, Muller R, Gronowicz G, Chorev M, Otu H, Libermann T, Alexander JM 2004 Differential transcriptional effects of PTH and estrogen during anabolic bone formation. J Cell Biochem 93:476–490. [PubMed: 15372627]
23. Iwaniec UT, Yuan D, Power RA, Wronski TJ 2006 Straindependent variations in the response of cancellous bone to ovariectomy in mice. J Bone Miner Res 21:1068–1074. [PubMed: 16813527]
24. Parfitt AM, Drezner MK, Glorieux FH, Kanis JA, Malluche H, Meunier PJ, Ott SM, Recker RR 1987 Bone histomorphometry: Standardization of nomenclature, symbols, and units. Report of the ASBMR Histomorphometry Nomenclature Committee. J Bone Miner Res 2:595–610. [PubMed: 3455637]
25. Kostenuik PJ, Harris J, Halloran BP, Turner RT, Morey-Holton ER, Bikle DD 1999 Skeletal unloading causes resistance of osteoprogenitor cells to parathyroid hormone and to insulin-like growth factor-I. J Bone Miner Res 14:21–31.
26. Iida-Klein A, Lu SS, Cosman F, Lindsay R, Dempster DW 2007 Effects of cyclic vs. daily treatment with human parathyroid hormone (1–34) on murine bone structure and cellular activity. Bone 40:391–398. [PubMed: 17056311]
27. Yamaguchi M, Ogata N, Shinoda Y, Akune T, Kamekura S, Terauchi Y, Kadowaki T, Hoshi K, Chung UI, Nakamura K, Kawaguchi H 2005 Insulin receptor substrate-1 is required for bone anabolic function of parathyroid hormone in mice. Endocrinology 146:2620–2628. [PubMed: 15718274]
28. Shinar DM, Endo N, Halperin D, Rodan GA, Weinreb M 1993 Differential expression of insulin-like growth factor-I (IGF-I) and IGF-II messenger ribonucleic acid in growing rat bone. Endocrinology 132:1158–1167. [PubMed: 8440176]
29. Iwaniec TUWT, Liu J, Rivera MF, Arzaga RR, Hansen G, Brommage R 2007 Parathyroid hormone stimulates bone formation in mice deficient in Lrp5. J Bone Miner Res 22:394–402. [PubMed: 17147489]
30. Wang Y, Sakata T, Elalieh HZ, Munson SJ, Burghardt A, Majumdar S, Halloran BP, Bikle DD 2006 Gender differences in the response of CD-1 mouse bone to parathyroid hormone: Potential role of IGF-I. J Endocrinol 189:279–287. [PubMed: 16648295]
31. Lazowski DA, Fraher LJ, Hodsman A, Steer B, Modrowski D, Han VK 1994 Regional variation of insulin-like growth factor-I gene expression in mature rat bone and cartilage. Bone 15:563–576. [PubMed: 7980968]
32. Locklin RM, Khosla S, Turner RT, Riggs BL 2003 Mediators of the biphasic responses of bone to intermittent and continuously administered parathyroid hormone. J Cell Biochem 89:180–190. [PubMed: 12682918]
33. Knopp E, Troiano N, Bouxsein M, Sun BH, Lostritto K, Gundberg C, Dziura J, Insogna K 2005 The effect of aging on the skeletal response to intermittent treatment with parathyroid hormone. Endocrinology 146:1983–1990. [PubMed: 15618351]
34. Suda T, Takahashi N, Udagawa N, Jimi E, Gillespie MT, Martin TJ 1999 Modulation of osteoclast differentiation and function by the new members of the tumor necrosis factor receptor and ligand families. Endocr Rev 20:345–357. [PubMed: 10368775]
35. Miyamoto T, Suda T 2003 Differentiation and function of osteoclasts. Keio J Med 52:1–7. [PubMed: 12713016]

36. Boyle WJ, Simonet WS, Lacey DL 2003 Osteoclast differentiation and activation. Nature 423:337–342. [PubMed: 12748652]

37. Huang JC, Sakata T, Pfleger LL, Bencsik M, Halloran BP, Bikle DD, Nissenson RA 2004 PTH differentially regulates expression of RANKL and OPG. J Bone Miner Res 19:235–244. [PubMed: 14969393]

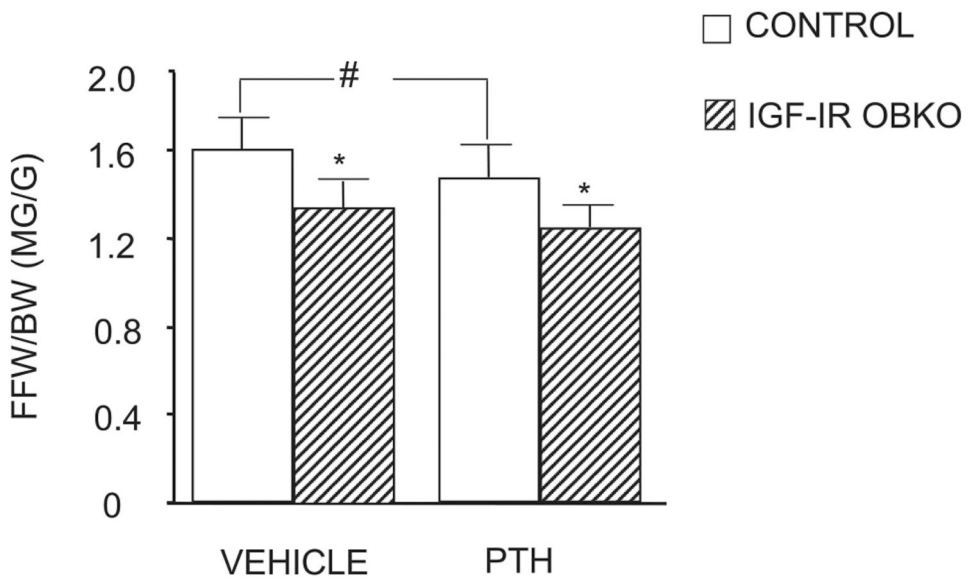

FIG. 1.

IGF-IR is required for the actions of PTH on bone mass. Fat-free weight/body weight (FFW/BW) of tibia in IGF-I receptor osteoblast null (IGF-IR OBKO, hatched bars) mice was significantly less ($^{*}p < 0.05$) than that in control mice (open bars). PTH significantly ($^{\#}p < 0.05$) decreased FFW/BW of tibia in control mice, but not in IGF-IR OBKO mice, although the same trend was observed. Results are expressed as means ± SD: $n = 7$ (four males and three females) in the vehicle-treated control group and $n = 9$ (four males and five females) in the other groups.

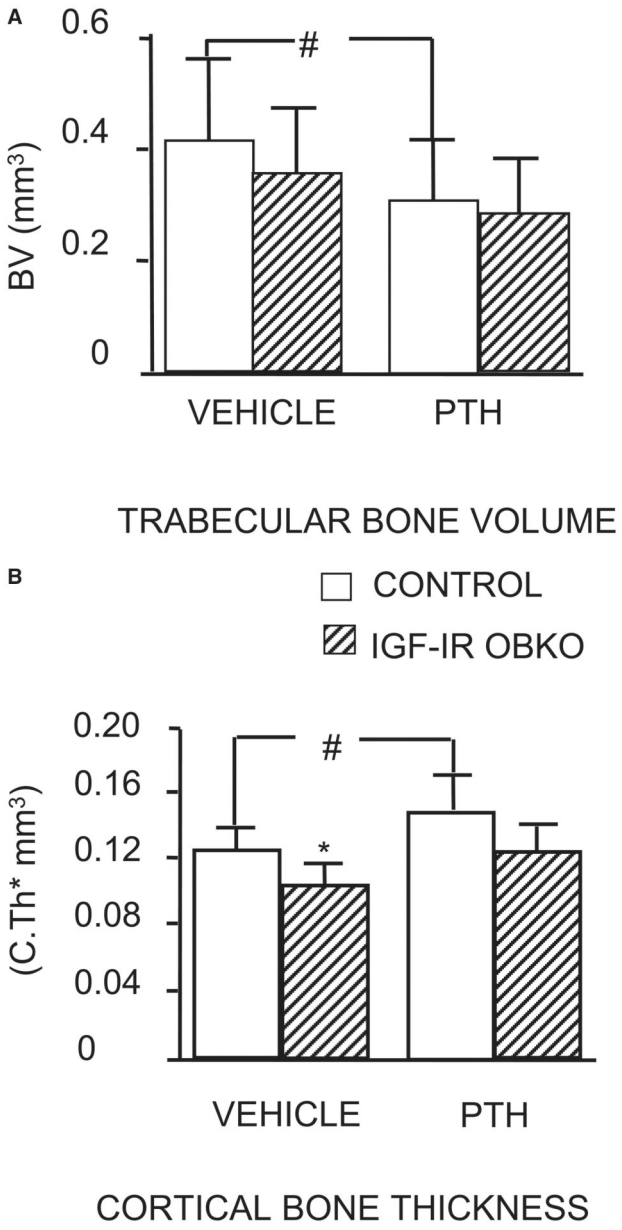

FIG. 2.

Role of *IGF-IR* in mediating the response of PTH on bone structure. Trabecular bone volume (BV) and cortical bone thickness (C. Th; $*p < 0.05$) were less in IGF-I receptor osteoblast null (IGF-IR OBKO) mice (hatched bars) than in control mice (open bars). PTH significantly decreased BV by 22% ($^{\#}p < 0.05$) and increased C.Th by 18% ($^{\#}p < 0.05$) in control mice, but had less effect in IGF-IR OBKO mice, although the trends were comparable. Results were determined by μCT and expressed as means ± SD: $n = 7$ (four males and three females) in the vehicle-treated control group and $n = 9$ (four males and five females) in the other groups.

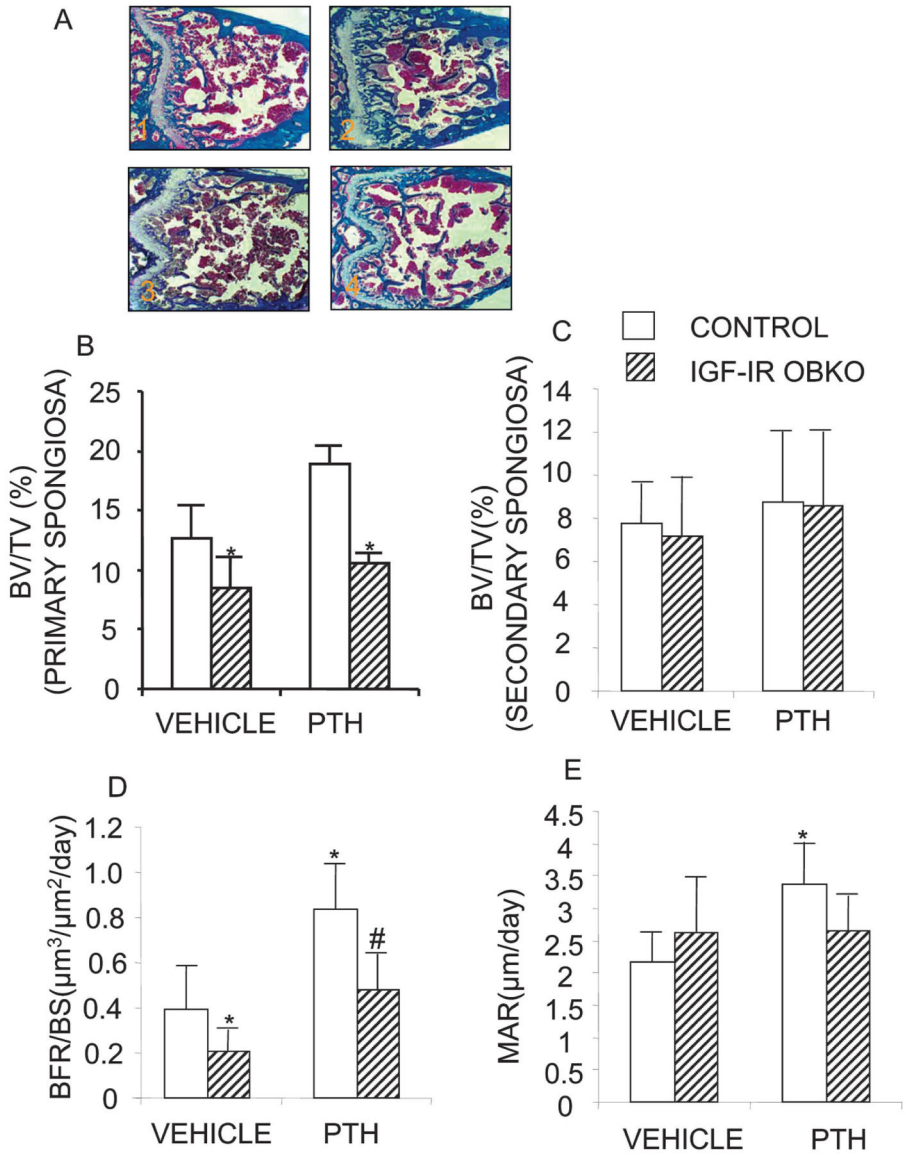

FIG. 3.

Role of *IGF-IR* in mediating the response of PTH on trabecular bone volume and formation. At the primary spongiosa, trabecular bone volume (BV/TV; $*p < 0.05$) was less in IGF-IR OBKO mice (A3, hatched bars in B) than in control mice (A1, open bars in B). PTH significantly increased BV/TV control mice (A2, open bars in B), but had less effect at the primary spongiosa of IGF-IR OBKO mice (A4, hatched bars in B). At the secondary spongiosa, PTH had less effect on BV/TV of both control (C, open bars) and IGF-IR OBKO (C, hatched bars). Trabecular bone formation rate (BFR/BS) significantly ($*p < 0.05$) decreased in the IGF-IR OBKO mice (D, hatched bars) than control mice (D, open bars). PTH stimulated BFR/BS in both control mice ($*p < 0.05$) and IGF-IR OBKO mice ($^{\#}p < 0.05$). There were no significant differences on mineral apposition rate (MAR) between control mice (E, open bars) and IGF-IR OBKO mice (E, hatched bars). PTH stimulated MAR only in the control mice ($*p < 0.05$). Results were determined by bone

histomorphometry, expressed as means ± SD: $n = 8$ (four males and four females) in each group.

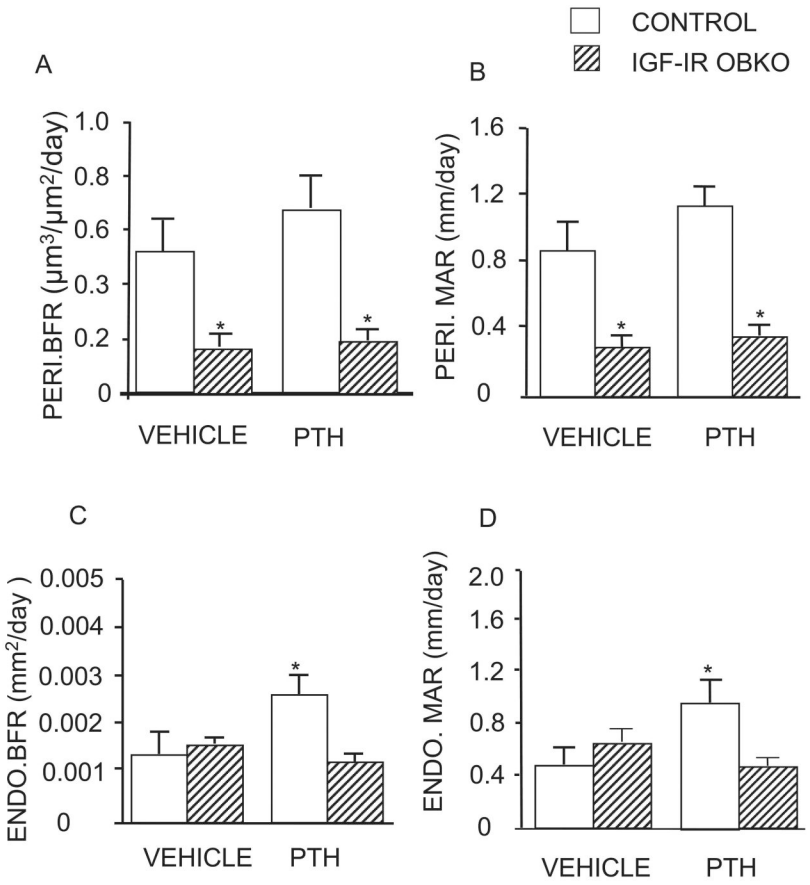

FIG. 4.

IGF-IR mediates the stimulation by PTH of periosteal and endosteal bone formation at the tibiofibular junction (TFJ). Periosteal bone formation rate (Peri. BFR) (A) and mineral apposition rate (Peri. MAR) (B) were significantly lower in IGF-I receptor osteoblast null mice (IGF-IR OBKO, hatched bars) than in control mice (open bars). PTH tended to increase Peri.BFR (A) and Peri.MAR (B) in control mice ($p = 0.58$), but had no effect in the IGF-IR OBKO mice. Endosteal (Endo.) BFR (C), and MAR (D) were comparable in control and IGF-IR OBKO mice. PTH significantly increased Endo.BFR and Endo.MAR in control mice but not in IGF-IR OBKO mice. Results were determined by bone histomorphometry using double label tetracycline and expressed as means ± SD. *$p < 0.05$ vs. vehicle-treated control mice. $n = 7$ (four males and three females) in the vehicle-treated control group and $n = 9$ (four males and five females) in the other groups.

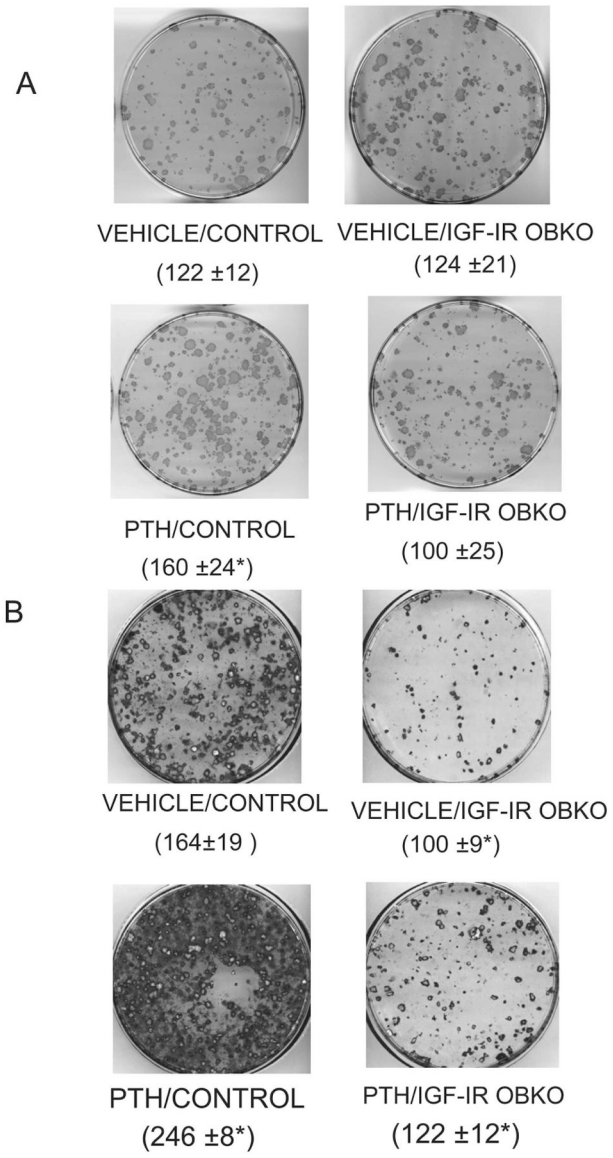

FIG. 5.

IGF-IR is required for PTH to stimulate osteoprogenitor cell proliferation and differentiation. The numbers of ALP^+ colonies at day 14 of culture are equivalent in BMSCs from IGF-I receptor osteoblast null (IGF-IR OBKO) mice and controls. However, PTH increased the number of these colonies only in the controls (A). Subsequent mineralization (calcium nodules staining by alizarin red) of these colonies from the IGF-IR OBKO mice by day 28 was markedly decreased. PTH significantly increased mineralization on day 28 in BMSCs from control mice but not in BMSCs from IGF-IR OBKO mice. Results are expressed as means ± SD. *$p < 0.05$ vs. vehicle-treated control mice. $n = 4$ (three males and one female) in the vehicle-treated control and IGF-IR OBKO mice; $n = 6$ (three males and three females) in PTH-treated control mice; and $n = 5$ (three males and two females) in PTH-treated IGF-IR OBKO mice.

TABLE 1.

REAL-TIME PCR RESULTS

Group	IGF-I	RUNX2	AP	OCN	RANKL
Control/vehicle	3.99 ± 0.20	4.16 ± 2.96	38.4 ± 16.41	198.96 ± 118.77	0.38 ± 0.02
Control/PTH	6.47 ± 0.32*	22.36 ± 0.42*	208.09 ± 41.42*	964.51 ± 33.5*	8.39 ± 1.05*
IGF-IR OBKO/vehicle	5.26 ± 0.26*	3.18 ±2.14	33.54 ± 14.84	113.55 ± 43.46*	0.65 ± 0.55
IGF-IR OBKO/PTH	3.24 ± 0.16*	3.08 ± 1.16*	40.61 ± 1.11	158.40 ± 90.89	1.51 ± 0.07

Results are assessed by real-time PCR and expressed as percentage of GAPDH expression control (means ± SD).

$n = 4$ in vehicle-treated control mice and IGF-IR OBKO mice and $n = 5$ in PTH-treated control and IGF-IR OBKO mice.

* $p < 0.05$ vs. vehicle-treated control mice.